MWCNTs-supported Ni electrocatalyst-modified CPE as a sensing platform for voltammetric determination of ibuprofen in pharmaceutical formulations

Ana D. Đurović[1] · Vuk V. Gudelj[1] · Sanja N. Panić[2] · Snežana Ž. Kravić[1] · Lukáš Richtera[3,4] · Zorica S. Stojanović[1]

Abstract

In this work, a sensitive and reproducible voltammetric methodology using a modified carbon paste electrode has been established for the determination of the non-steroidal anti-inflammatory drug ibuprofen. MWCNTs-supported Ni electrocatalyst was applied as a bulk carbon paste modifier to fabricate the Ni-MWCNTs-CPE sensor, while square-wave voltammetry was utilized as an electroanalytical technique. Besides, cyclic voltammetry was used to study the electrochemical behavior of ibuprofen on the proposed sensor. Parameters of square-wave voltammetry were optimized using acetate buffer pH 4.5 as an optimal electrolyte. In addition, the sensitivity of the modified carbon paste electrode, as a sensing element, was compared to the unmodified one. Under optimized conditions, a wide linear range was obtained with *LOD* and *LOQ* values of 0.86 and 2.61 μM, and 0.13 and 0.39 μM, for bare CPE and Ni-MWCNTs-CPE, respectively. The presence of the modifier in the paste improved the sensitivity of the carbon paste electrode by almost 7 times. In addition, the newly fabricated Ni-MWCNTs-CPE sensor showed better results in terms of precision (RSD up to 2.49%). Finally, the validated voltammetric methodology was successfully applied for the determination of ibuprofen content in pharmaceutical formulations, without any complicated preliminary preparation steps, with recovery values between 94.4 and 98.1%.

Graphical abstract
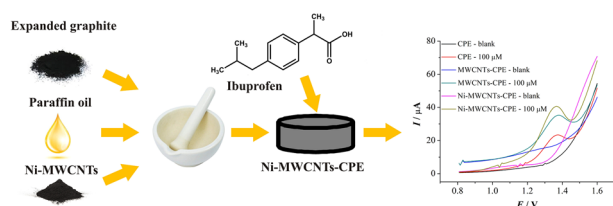
Keywords Sensors · Voltammetry · Electrochemistry · Carbon paste electrode · Modification

✉ Ana D. Đurović
  ana.djurovic@uns.ac.rs

1 Faculty of Technology Novi Sad, Department of Applied and Engineering Chemistry, University of Novi Sad, Bulevar cara Lazara 1, 21000 Novi Sad, Serbia

2 Faculty of Technology Novi Sad, Department of Basic Engineering Disciplines, University of Novi Sad, Bulevar cara Lazara 1, 21000 Novi Sad, Serbia

3 Department of Chemistry and Biochemistry, Mendel University in Brno, Zemědělská 1, 613 00 Brno, Czech Republic

4 Central European Institute of Technology, Brno University of Technology, Purkyňova 123, 612 00 Brno, Czech Republic

Introduction

Non-steroidal anti-inflammatory drugs (NSAIDs) are one of the most dominant groups of pharmaceutical substances used for the treatment of patients suffering from pain and various inflammatory conditions. Ibuprofen ((*RS*)-2-[4-(2-methylpropyl)phenyl]propanoic acid, IBU, Fig. 1), a typical representative of NSAIDs, combines anti-inflammatory, analgesic, and antipyretic activities [1]. Since its discovery for the treatment of rheumatoid arthritis, IBU has been one of the best-selling drugs worldwide [2]. It is widely used for
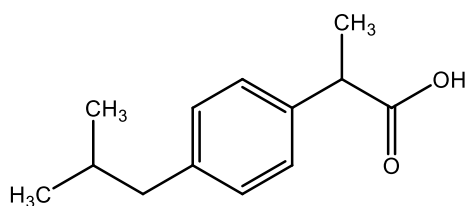
Fig. 1 Chemical structure of ibuprofen

the treatment of various pain states (dental, dysmenorrhoea, sports injuries), joint inflammation, and arthritis pain [3], although recent studies demonstrated its potential beneficial effects in numerous chronic inflammatory and degenerative diseases, as well as in some cancers [1]. As a drug of relatively low systemic toxicity, cases of IBU poisoning are rare with either asymptomatic or mild gastrointestinal symptoms, and rare incidence of death in case of exceeding the maximum daily dose of 2400 mg [4, 5]. Yet, to avoid adverse reactions and ensure sufficient effective dosage, it is inevitable to develop fast and easily available analytical methods for the precise determination of this drug in various real samples, including various forms of pharmaceutical formulations.

In the recent past for the determination of IBU, conventional analytical methodologies have dominated including chromatographic methods such as gas chromatography [6, 7] and high-performance liquid chromatography [8–12], capillary electrophoresis [13] and spectroscopy [14]. The principles of these methodologies are well established, and they provide reliable results in the analysis of real samples with low *LOD*s, along with the requirements of sophisticated equipment and highly trained personnel. However, the modern age imposes new requirements on up-to-date analytics, directing it towards direct analysis without sample preparation in a short time and the use of expeditious methods which imply a lower volume of hazardous and toxic chemicals.

Electroanalytical methods have repeatedly proven very promising in the field of drug analysis in pharmaceuticals and various real samples [15–17]. Apart from high sensitivity accompanied by sufficient selectivity, accuracy, and short analysis time, electroanalytical techniques do not require toxic reagents and well-trained staff [18, 19]. Generally, with the use of very sensitive pulse voltammetric methods combined with nanomaterials of the new generation as sensing electrode material, it is possible to approach detection limit values typical for chromatographic techniques by skipping tedious and time-consuming sample pretreatment. One of the promising groups of nanomaterials is carbon nanotubes. Designed as graphite sheets rolled into cylindrical shapes, two types of these materials are distinguished: single-walled carbon

nanotubes (SWCNTs) consist of a single graphene layer, and multi-walled carbon nanotubes (MWCNTs) comprised of two or several cylinders made of graphene sheets [20]. Owing to their exceptional physical and chemical properties including high tensile strength, ultra-lightweight and high chemical and thermal stability, interest in the application of these attractive materials is increasing [20]. Combining the advantages of these materials, analysts have been able to improve sensor performance through modification processes which resulted in the improvement of the electron transfer, as well as increasing the peak current of a targeted molecule on the surface of the carbon nanotube-modified electrodes.

In this work, the application of carbon nanomaterial in order to upgrade the sensor's performance through the modification process is described. In fact, MWCNTs-supported Ni electrocatalyst (Ni-MWCNTs) was synthesized for this purpose, and incorporated into the carbon paste as a bulk modifier. Subsequently, the performance of the modified carbon paste electrode (Ni-MWCNTs-CPE) was compared with the unmodified one, resulting in improved sensitivity and significantly better accuracy.

Results and discussion

SEM and EDS characterization of synthesized MWCNTs samples and Ni-MWCNTs

The morphology of synthesized MWCNTs samples (pristine and purified), as well as the Ni-MWCNTs as the electrocatalyst, was characterized by SEM as shown in Fig. 2. The corresponding EDS spectra were presented as inset images. SEM image of pristine MWCNTs revealed the high selectivity of multi-walled carbon nanotube formation over 5% Fe–Co/Al_2O_3 catalyst, indicating a homogeneous and dense distribution of the tubes covering the catalyst surface in a web-like network. The catalyst particles are clearly visible and the elemental composition of the sample was confirmed by EDS analysis. After the purification treatment, the catalyst remains were almost completely removed, while the morphology of the tubes can be portrayed by highly interwoven and twisted structures, denser compared to the pristine sample (Fig. 2b). Due to the low magnification of the applied SEM equipment, Ni particles present in the electrocatalyst could not be detected, implying that their size is too small to be clearly visible, accompanied with their distribution within the dense network of the tubes. However, the results from the corresponding EDS spectrum confirmed the presence of Ni with an average of 9.1 wt% (based on 5 measuring points), while carbon and oxygen are present in the sample with 80 wt% and 10.9 wt%, respectively.
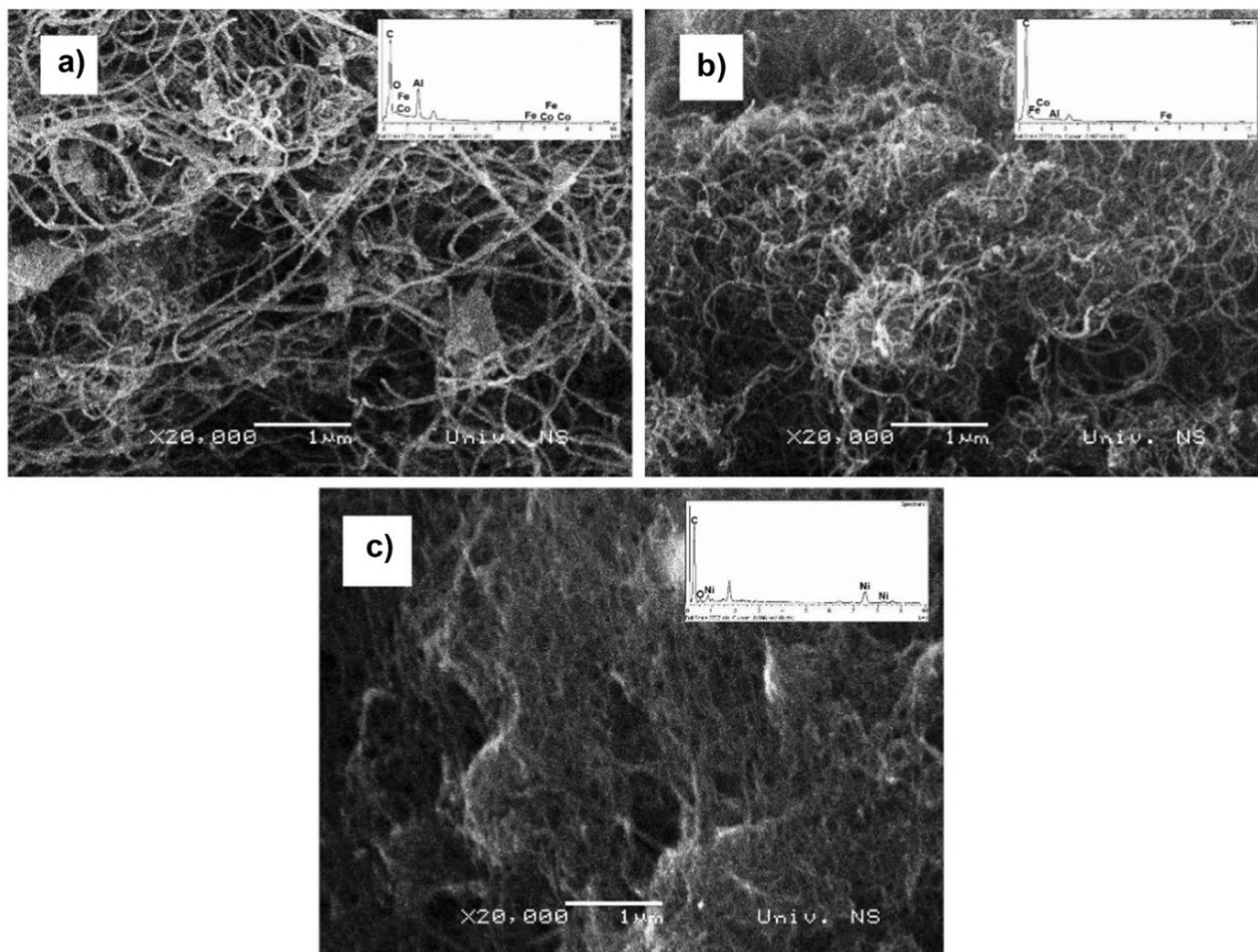
Fig. 2 SEM images with the inset of EDS spectra of the **a** MWCNTs synthesized over 5% Fe–Co/Al$_2$O$_3$ catalyst (pristine); **b** MWCNTs after the purification and **c** MWCNTs-supported Ni electrocatalyst

Electrochemical characterization of the modified electrode

The effect of the modification process of the bare CPE by Ni-MWCNTs was tested in terms of an improvement of the electrochemical properties of the modified electrode. To this end, the electrochemical behavior and electroactive surface area of bare CPE were compared with that of Ni-MWCNTs-CPE by performing CV measurements in a solution containing 5 mM of [Fe(CN)$_6$]$^{3-/4-}$ in 0.1 M KCl. In comparison to the bare CPE, Ni-MWCNTs-CPE provided a better defined reversible redox peak with a higher current signal (Fig. 3a). Further, the Randles–Sevcik equation was used for electroactive surface area estimation:

$$I_p = 2.69 \times 10^5 n^{3/2} A D^{1/2} \nu^{1/2} C_p \tag{1}$$

where I_p stands for the peak current (A), n is the number of transferred electrons, A is the effective surface area (cm^2),

D is diffusion coefficient (cm^2/s), ν is the potential scan rate (V s^{-1}), and C_p corresponds to the concentration of the redox probe (mol cm^{-3}) [21]. For the solution [Fe(CN)$_6$]$^{3-}$ in 0.1 M KCl, $n = 1$ and $D = 7.6 \times 10^{-6}$ cm^2 s^{-1} [22]. The calculated values of active surface area were 0.070 cm^2 and 0.094 cm^2 for CPE and Ni-MWCNT-CPE, respectively, indicating that the Ni-MWCNTs as the modifier increased the active electrode surface area by 34%.

In order to further characterize the working electrode before and after the modification process, electrochemical impedance spectroscopy (EIS) measurements were performed in the solution containing 5 mM [Fe(CN)$_6$]$^{3-/4-}$ in 0.1 M KCl, over a frequency range of 0.1 to 10^5 Hz, by applying a fixed potential of 200 mV and signal amplitude of 10 mV (Fig. 3b). Nyquist plots consisted of a semicircular and a linear part. The electron transfer resistance (R_{ct}) at the electrode surface is related to the semicircle diameter of the Nyquist plot.

Electrochemical behavior of IBU at CPE, MWCNTs-CPE, and Ni-MWCNTs-CPE
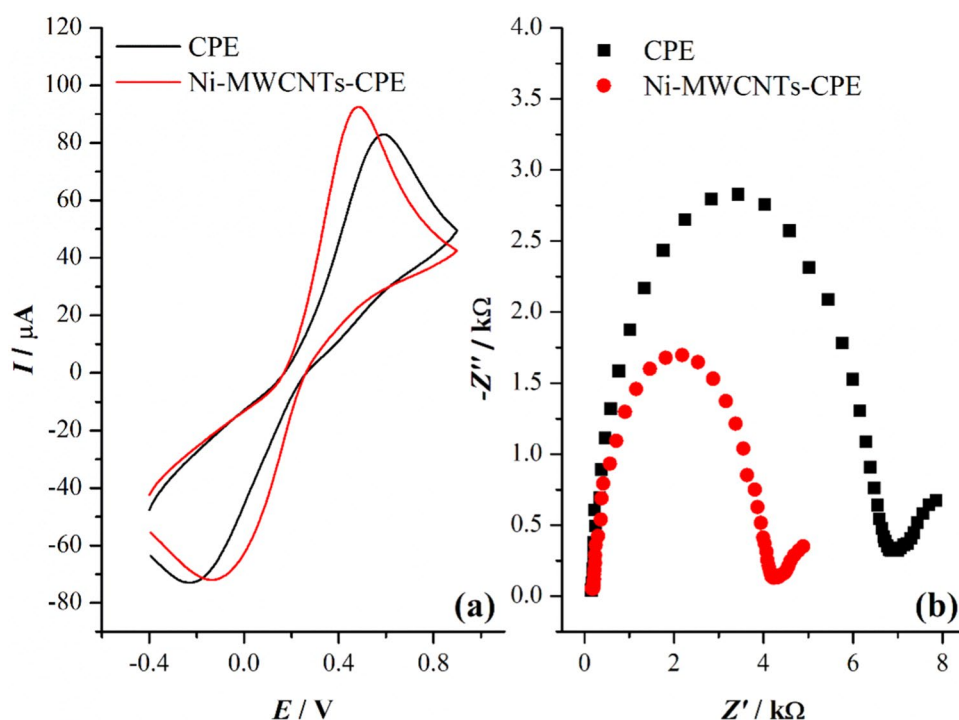
Obviously, the semicircle diameter of the working electrode was decreased by implementing a Ni-MWCNTs material as a modifier in the paste. The experimental EIS data were fitted using standard Randle's equivalent circuit [$R(C[RW])$], where the resistance to charge transfer (R_{ct}) and the Warburg impedance (W) were both in parallel with the double-layer capacitance (C). By fitting the data, estimated R_{ct} values were 6185 Ω and 3766 Ω for bare and modified CPE, respectively, demonstrating that Ni-MWCNTs as a material used for modification accelerates the electron transfer between the electrode surface and the analyte.

During preliminary experiments, the feasibility of voltammetric measurements using CPE, MWCNTs-CPE, and Ni-MWCNTs-CPE as a sensor and IBU as a targeted analyte was investigated in 0.1 M acetate buffer pH 4.5. SWV voltammograms of IBU (100 μM) were registered at bare CPE, MWCNTs-CPE, and Ni-MWCNTs-CPE for comparison (Fig. 4). One clearly visible oxidation peak appears at all three sensors, indicating irreversible oxidation of the analyte. The IBU oxidation peak exhibited a relatively broad and weak appearance on the bare CPE. The incorporation of MWCNTs in the paste induced a shift in the baseline, along with amplification of the IBU oxidation peak. The most distinct voltammogram, displaying the highest current response, was observed on the Ni-MWCNTs-CPE,
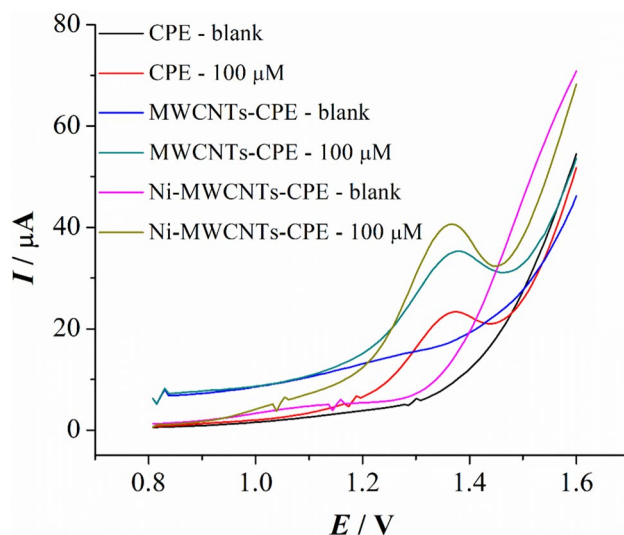

Fig. 4 Responses of bare CPE, MWCNTs-CPE, and Ni-MWCNTs-CPE during the voltammetric determination of IBU using SWV ($E_{SW} = 50$ mV, $f = 50$ Hz, $\Delta E = 7.5$ mV, $t_{eq} = 5$ s) in acetate buffer pH 4.5. $C_{IBU} = 100$ μM

indicating a synergistic effect between nickel particles and MWCNTs.

Supporting electrolyte and pH value

Towards upgrading sensors' performance by the chemical composition of the optimal supporting electrolyte, the SWVs were recorded using different buffers. Phosphate pH 6.0,

acetate pH 4.5, Britton–Robinson pH 6.0, and citrate buffers pH 6.0 were compared with respect to the response toward IBU (100 μM) on CPE and Ni-MWCNTs-CPE. The best signal for both sensors was obtained by utilizing an acetate buffer. The electrochemical inquiry of 200 μM IBU in 0.1 M acetate buffer at CPE and Ni-MWCNTs-CPE was studied in the pH range between 3.5 and 5.5 (Fig. 5).

The oxidation peak current and peak potential values varied with the pH values of the acetate buffer. The peak current of IBU reached a maximum at pH 4.5 on both sensors. The obtained results are in agreement with other studies in which a pH of 4.5 or 5 was found to be optimal for IBU oxidation [23–25]. The increase in pH value results in the negative shift of peak potential, demonstrating a proton-involved electrode reaction.

The plots of peak potential (E_p) vs. pH solution value showed linear relationships, with slope values of -0.0550 and -0.0632 for CPE and Ni-MWCNTs-CPE, respectively, which are close to the Nernstian theoretical value of -0.059, indicating on an equal number of protons and electrons transferred in the redox reaction of IBU on the surface of electrodes [26].

Optimization of the modified sensor composition

Since the composition of the carbon paste largely determines the response of the working electrode, by determining the rate of the electron transfer, as well as the background current, the optimal amount of the particular modifier Ni-MWCNTs was ascertained in the carbon paste. The optimization of the modifier quantity was achieved by crafting the sensors using three different percentages: 2.5%, 5%, and 10% of the modifier (*w/w* relative to the mass of the solid phase). These percentages are commonly found in the literature for bulk modification [27]. During the SW voltammetry experiments, the response of the modified electrode was closely monitored for an IBU concentration of 100 μM, and the detailed results can be found in the supplementary material (Fig. 1S). An increase in the amount of modifier in the paste, ranging from 2.5% to 5%, led to an observable
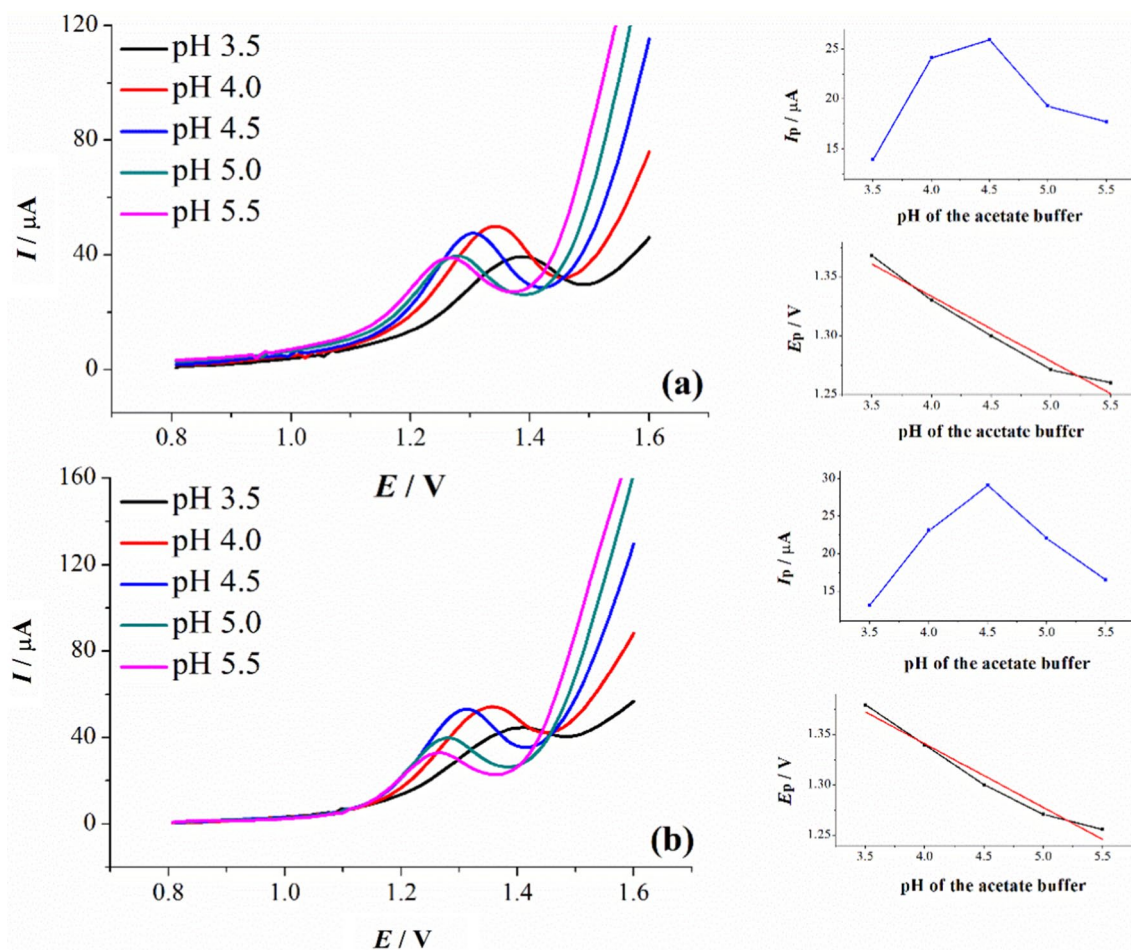

Fig. 5 SWVs of IBU ($E_{SW}=50$ mV, $f=50$ Hz, $\Delta E=7.5$ mV, $t_{eq}=5$ s) in 0.1 M acetate buffer at pH 3.5, 4.0, 4.5, 5.0, and 5.5 at: **a** CPE and **b** Ni-MWCNTs-CPE. Insets: plots I_p (up) and E_p (down) vs. pH of the acetate buffer. $C_{IBU}=200$ μM

enhancement in the signal. However, when the modifier content was further increased to 10%, there was a reduction in the IBU signal. Consequently, a modifier concentration of 5% was deemed optimal, aligning with the results.

Scan rate study

Scan rate has an important role in identifying the reaction mechanism of IBU at the applied sensor. Accordingly, the response of 100 μM IBU was observed at various scan rates (ν) in the range of 10–500 mV s^{-1} by CV at bare CPE and Ni-MWCNTs-CPE. By plotting the current peaks (I_p) vs. the square root of the scan rate ($\nu^{1/2}$) linear graphs were obtained for CPE and Ni-MWCNTs-CPE, respectively (Fig. 6), indicating that the oxidation of IBU on the surface of the electrode is controlled by diffusion. Moreover, linear correlations were derived by drawing the logarithm of the current peak (log I_p) vs. those of scan rates (log ν) according to the equations presented in Fig. 6, with slope values

of 0.5433 and 0.6596. A slope value of 0.5433, obtained for CPE, closely approximates the theoretical value of 0.5, suggesting a diffusion-dominated process [28]. However, in the case of the modified electrode, the slightly higher slope value suggests that the oxidation process of IBU does not adhere strictly to either diffusion or adsorption control.

Furthermore, a shift towards more positive anodic peak potentials as the scan rate increased is observed (the results are not shown). This shift is a confirmation of the irreversibility of the IBU oxidation process. Using the data available in this study, it is possible to calculate the number of electrons engaged in the IBU oxidation reaction. This calculation can be executed according to Laviron's theory [29]. For the irreversible redox reaction, the number of electrons participating in the oxidation of IBU can be ascertained by examining the linear relationship between the anodic peak potential (E_p) and the natural logarithm of the scan rate (ln ν) using the following equation:
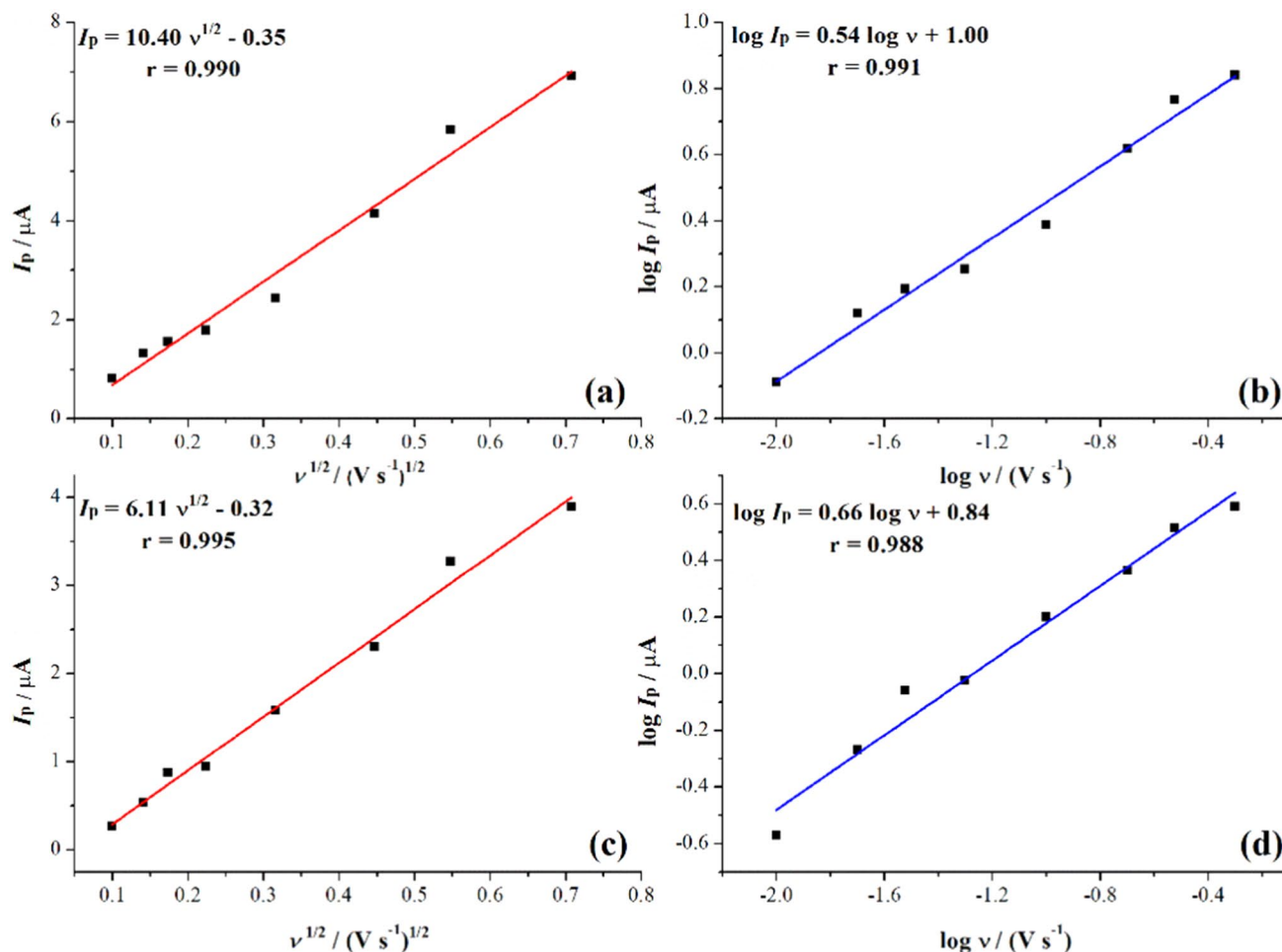
Fig. 6 The dependences of the peak current (I_p) of IBU on the square root of the potential scan rate (ν)$^{1/2}$ for **a** CPE and **c** for Ni-MWCNTs-CPE; the dependences of the logarithm of the peak current (log I_p) of IBU on the logarithm of the potential scan rate (log ν) obtained for **b** CPE and **d** Ni-MWCNTs-CPE. The scan rate varied in the range of 0.01–0.5 V s^{-1}. $C_{IBU} = 100$ μM in acetate buffer pH 4.5

$$E_p = E° + \left(\frac{RT}{\alpha nF}\right) \ln\left(\frac{RTk°}{\alpha nF}\right) + \left(\frac{RT}{\alpha nF}\right)\ln\nu \qquad (2)$$

Here, E_p signifies the peak potential relative to a reference electrode, $E°$ represents the formal potential, T designates the temperature (298.15 K), F denotes the Faraday constant (96,485 C mol^{-1}), R is the universal gas constant (8.314 K mol^{-1}), n refers to the number of transferred electrons, α characterizes the charge transfer coefficient for the oxidation step, $k°$ stands for the heterogeneous rate constant (s^{-1}), and ν indicates the scan rate (V s^{-1}). The slope value of 0.0264, derived from the regression equation of E_p vs. (ln ν) for Ni-MWCNTs-CPE, aligns with $RT/\alpha nF$. Based on this slope value, the αn value is determined to be 0.973. Assuming an α value of 0.5, it can be inferred that two electrons are engaged in the irreversible redox reaction. Conversely, comparable findings, signifying the exchange of two electrons during the IBU oxidation process, were also evident in a study employing a boron-doped diamond electrode [30]. This study provides a comprehensive elucidation of the IBU oxidation mechanism.

Optimization of the instrumental parameters

To enhance the performance of the CPE and Ni-MWCNTs-CPE sensors for voltammetric determination of IBU, instrumental parameters such as pulse amplitude (E_{sw}), frequency (f), step potential (ΔE), and equilibrium time (t_{eq}) were optimized. Consequently, the SW voltammograms in the presence of 100 μM IBU were recorded by varying the values of E_{sw} (10–200 mV), f (10–100 Hz), ΔE (1–20 mV), and t_{eq} (0–20 s), by modifying one parameter at a time, in order to obtain the highest and most refined voltammograms. The increase in the pulse amplitude leads to an increase in peak current, but this parameter also influences the peak shape. Thus, the IBU peaks become wider with higher values of E_{sw}.

The same was observed in the case of increasing frequency, leading to an increase in the analytical signal; however, at certain values, the noise was increased as well. In the case of step potential investigation, increasing the value led to signal intensification, but also protracted IBU peaks, while no significant changes were observed with variation of the t_{eq} values. Consequently, the compromise between sensitivity and peak appearance was fulfilled by following the next parameters: E_{sw} of 75 mV, f of 50 Hz, ΔE of 7.5 mV, and t_{eq} of 10 s, for both sensors (Figs. 2–3S).

Calibration curves

The quantification capability of the herein-prepared carbon paste sensors was demonstrated by recording SWVs of increasing concentrations of IBU in 0.1 M acetate buffer pH 4.5, as shown in Fig. 7. Under optimized parameters, the relationship between the peak current (I_p) and IBU concentration (c_{IBU}) was studied in the range of 10–500 μM. The obtained calibration plots presented two linear ranges from 10 to 100 μM, and from 100 to 500 μM for CPE, while for Ni-MWCNTs-CPE, linear ranges were obtained from 25 to 100 μM, and from 100 to 500 μM (Fig. 7). The linear dependence was expressed by the regression equations presented in Fig. 7, with the correlation coefficients close to 1, indicating good linearity of calibration dependences obtained by both sensors.

The limit of detection (*LOD*) and limit of quantification (*LOQ*) were calculated according to the following equations [31, 32]:

$$LOD = 3.3S_b/b \qquad (3)$$

$$LOQ = 10S_b/b \qquad (4)$$

where S_b is the standard deviation of the y-intercept obtained from the line for the lower concentration range, and b is the slope of this line. The reported values of *LOD* and *LOQ* were 0.86 and 2.61 μM, and 0.13 and 0.39 μM, for CPE and Ni-MWCNTs-CPE, respectively. Although in the case of the bare CPE, a wider linearity range was obtained, the addition of the modifier to the paste lowered the *LOD* value by almost 7 times. In comparison with the performance of sensors based on carbon paste electrodes developed for IBU determination [33–36], the results obtained within this work showed comparable characteristics (Table 1).

Precision

The precision of the described methodologies was estimated through repeatability and reproducibility testing and calculating derived RSD values. The repeatability was studied by performing ten voltammetric analyses while detecting 50 and 100 μM of IBU during the same day under the optimized conditions established for CPE and Ni-MWCNTs-CPE (Table 1S).

Maximum RSD values of the peak current were calculated for CPE to be 2.30%. The reproducibility assay was performed by analyzing the same IBU concentrations for three days using both sensors, and the results gave a maximum RSD value for CPE of 2.49%. The results obtained within this part of the experiments revealed the significantly better performance of the modified electrode with lower RSD values in relation to the unmodified electrode.

Analytical application

In order to verify the practical applicability of the presented sensors in real samples, CPE and Ni-MWCNTs-CPE
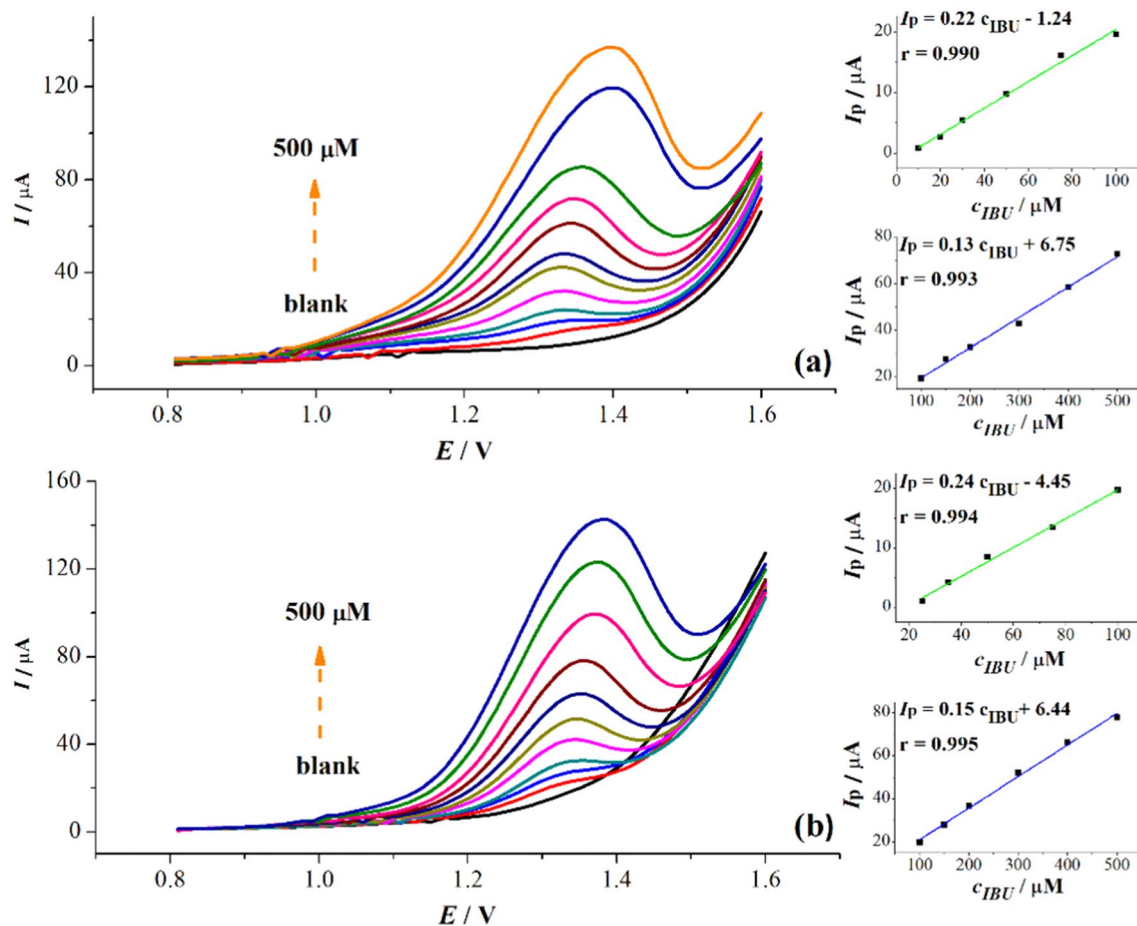
Fig. 7 SWVs of IBU in 0.1 M acetate buffer (pH = 4.5) at **a** CPE (C_{IBU} 10, 20, 30, 50, 75, 100, 150, 200, 300, 400, 500 μM) and **b** Ni-MWCNTs-CPE (C_{IBU} 25, 30, 50, 75, 100, 150, 200, 300, 400, 500 μM). Insets: corresponding calibration curves (E_{SW} = 75 mV, f = 50 Hz, ΔE = 7.5 mV, t_{eq} = 10 s)

Table 1 Comparison of the performances of CPE and Ni-MWCNTs-CPE with other CPE-based sensors using voltammetric techniques

Electrode	Linear range/M	*LOD*/M	Real sample	References
Pd–PdO/Mt–CPE	1.0×10^{-8}–1.0×10^{-6}	2.85×10^{-9}	Blood sample	[35]
Mt–CPE	1.0×10^{-7}–1.0×10^{-3}	6.80×10^{-8}	River water, commercial tablets	[36]
CPE-Clay	1.0×10^{-6}–1.0×10^{-3}	3.23×10^{-8}	Blood sample	[33]
MWCNTs-CPE	2.36×10^{-6}–242×10^{-6}	9.10×10^{-6}	Tablets	[34]
CPE	1.0×10^{-5}–5.0×10^{-4}	8.61×10^{-7}	Pharmaceutical formulations	This study
Ni-MWCNTs-CPE	2.5×10^{-5}–5.0×10^{-4}	1.28×10^{-7}	Pharmaceutical formulations	This study

Pd–PdO/Mt–CPE—palladium–palladium oxide particles montmorillonite CPE; Mt–CPE—montmorillonite-doped CPE; CPE-Clay—CPE-modified with clay; MWCNTs-CPE—CPE multi-walled carbon nanotube composite electrode; Ni-MWCNTs-CPE—multi-walled carbon nanotubes supported Ni electrocatalyst CPE

were utilized for detecting IBU in commercially available pharmaceutical formulations. Each sample was measured 3 times using SWV under the optimized conditions. Quantification of IBU was performed by the standard addition method with sufficient selectivity of the SWV technique allowing the IBU analytical signal to be distinguished from the interference excipients presented in the pharmaceuticals (Fig. 4S). The recovery and RSD results of the samples ranged between 94.4% and 98.1%, and 0.56–3.17%, respectively (Table 2), indicating the feasibility of the presented methodologies for precise and accurate quantification of IBU in pharmaceuticals.

Table 2 Determination of IBU in pharmaceutical formulations by standard addition method

Samples	Taken/mg	Found/mg[a]	Recovery/%	RSD/%
CPE				
Brufen tablets	200	196.2	98.1	3.17
Metafex tablets	200	194.8	97.4	1.55
Nurofen syrup[b]	200	191.1	95.6	0.90
Ni-MWCNTs-CPE				
Brufen tablets	200	195.3	97.7	1.23
Metafex tablets	200	190.4	95.2	0.56
Nurofen syrup[b]	200	188.8	94.4	1.13

[a] $n = 3$

[b] mg/5 cm^3

Conclusion

Briefly, the optimized SW voltammetric method utilizing bare and modified carbon paste electrodes, reliable for ibuprofen determination in pharmaceutical formulations is described. Both sensors showed similar performance in terms of electrochemical behavior, instrumental parameters, and linearity range. However, the application of the MWCNTs-supported Ni electrocatalyst, as a bulk carbon paste modifier, provided increased sensitivity and accuracy of the voltammetric method. The obtained values of *LOD* using optimized voltammetric methodology were as follows 0.13 μM and 0.86 μM for utilizing MWCNTs-supported Ni electrocatalyst-modified carbon paste electrode and bare carbon paste electrode, respectively. Ultimately, the herein presented voltammetric methodologies using bare and modified carbon paste electrodes as sensors are reliable for the accurate determination of ibuprofen content in commercial formulations without extraction and separation steps that are common in chromatography.

Experimental

IBU drug substance (≥ 98% GC) was obtained from Sigma-Aldrich, St. Louis, Missouri, USA. Pharmaceutical formulations that contain IBU as an active compound include Brufen 200 mg film tablets (Famar A.V.E., Athens, Greece), Metafex 200 mg/325 mg paracetamol tablets (Pharmaceutical Works Polpharma S.A., Gdańsk, Poland), and Nurofen syrup 200 mg/5 cm^3 oral suspension (Reckitt Benckiser Healthcare, Slay, UK) were purchased from a local drugstore. Acetic acid, sodium acetate trihydrate, sodium hydroxide, potassium ferricyanide, potassium ferrocyanide, potassium chloride, and paraffin oil were obtained from Sigma-Aldrich (St. Louis, Missouri, USA), while expanded graphite was obtained from Graphite Tyn Ltd. (Tyn and Vltavou, Czech Republic).

IBU standard solution (1×10^{-2} M) was prepared by dissolving the appropriate amount of standard in 10% ethanol (v/v). Solutions with a lower IBU concentration were prepared by dilution of the respective standard solution with the supporting electrolyte. For the preparation of the supporting electrolyte acetate buffer (0.1 M), acetate acid was mixed with sodium acetate trihydrate, while the pH was adjusted using sodium hydroxide to cover the pH range from 3.5 to 5.5. Double-distilled water was used for the preparations of all solutions.

A PalmSens 4 potentiostat (GA Houten, Netherlands) operated by PSTrace software (version 5.8) was used for all electrochemical measurements. The device was coupled with a conventional three-electrode system containing a CPE as a working electrode (bare or modified), Ag/AgCl (KCl, 3.5 M) as a reference electrode, and a platinum wire as a counter electrode. The pH was measured with a HI-221 pH-meter (Hanna Instruments, Woonsocket, USA) equipped with a combined glass electrode P11 (Sentek, Springwood, Essex, UK). The structure and morphology of as-synthesized (pristine) and purified MWCNTs, as well as the MWCNTs-supported Ni electrocatalyst, were characterized by scanning electron microscope (SEM) JEOL JSM-6460LV (Tokyo, Japan) with additional quantitative analysis by energy-dispersive spectroscopy (EDS).

Synthesis of MWCNTs-supported Ni electrocatalyst

MWCNTs synthesis was carried out in an ethylene/nitrogen flow mixture (1:1) at 700 °C, for 1 h using an in situ pre-reduced 5% Fe–Co/Al$_2$O$_3$ catalyst in a homemade reactor setup [37, 38]. The obtained raw material was boiled under reflux for 6 h in diluted NaOH (6 M) and HCl (6 M) solutions, respectively, in order to remove the catalyst remains. The resultant sample was collected on a filter, rinsed with double-distilled water until neutral pH, and dried at 100 °C for 24 h. The obtained washed and dried tubes were used as electrocatalyst support for the immobilization of nickel precursor Ni(NO$_3$)$_2$·6H$_2$O (Centrohem, Serbia) in an aqueous solution. The MWCNTs-supported Ni catalyst (10 wt. % total metal loading) was prepared by wet impregnation method using ultrasound treatment and mechanical stirring for 3 h and 24 h, respectively, in order to intensively homogenize the obtained slurry. After drying, the obtained powder was treated at 400 °C in N$_2$ gas flow (110 cm^3 min^{-1}) for 3 h and reduced at 700 °C in hydrogen flow (110 cm^3 min^{-1}) for 1 h. According to the available literature [39, 40] during the final stage of preparing the MWCNTs-supported Ni catalyst, which involves high-temperature reduction, a temperature of 700 °C was selected to facilitate complete reduction and

the formation of nickel particles, as well as their interaction with the MWCNTs support.

Working electrodes preparation

The CPE was prepared by thoroughly mixing 0.1 g of expanded graphite with 60 mm^3 of paraffin oil in a mortar until a homogeneous paste was obtained. The obtained paste was incorporated into the Teflon holder (length of 8.0 cm, an inner diameter of 4.0 mm) with a copper wire as an inner electrical contact. The same procedure was used in the case of modified CPE, with the replacement of a certain part of the expanded graphite with a modifier: 2.5, 5, and 10% (w/w, relative to the total mass of the solid phase). Smoothing of the electrode surface was performed by polishing on filter paper. The fresh electrode surface was obtained by extracting a small amount of paste from the tip of the electrode and repeating the smoothing procedure.

Voltammetric measurements

Voltammetric measurements were accomplished by CV and SWV with CPEs. Unless otherwise stated, a 0.1 M acetate buffer pH 4.5 was used as the supporting electrolyte (15 cm^3). CVs were recorded from $+0.8$ V to $+1.6$ V at different scan rates. SWVs were registered in the same potential range at an amplitude of 75 mV, frequency of 50 Hz, step potential of 7.5 mV, and equilibrium time of 10 s.

Real samples

One IBU tablet (Brufen and Metafex), or 5 cm^3 volume of syrup (Nurofen), was dissolved in a 10% mixture of 0.1 M phosphate buffer pH 7.0 and ethanol (*v/v*) with sonication for 2 min to facilitate the dissolution process in a volumetric flask. The working solutions with an IBU concentration of 100 µM in 0.1 M acetate buffer pH 4.5 were prepared from stock solutions of each pharmaceutical formulation.

Supplementary Information The online version contains supplementary material available at https://doi.org/10.1007/s00706-023-03158-0.

Data availability The data that support the findings of this study are available from the corresponding author upon reasonable request.

References

1. Rainsford KD (2015) Pharmacology and toxicology of ibuprofen. In: Rainsford KD (ed) Ibuprofen discovery, development and therapeutics. Wiley, Chichester, p 132
2. Rainsford KD (2015) History and development of ibuprofen. In: Rainsford KD (ed) Ibuprofen discovery, development and therapeutics. Wiley, Chichester, p 1
3. Kean WF, Rainsford KD, Buchanan WW (2015) Therapeutics of ibuprofen in rheumatic and other chronic painful diseases. In: Rainsford KD (ed) Ibuprofen discovery, development and therapeutics. Wiley, Chichester, p 237
4. Sachs CJ (2005) Am Fam Physician 71:913
5. Wood D, Monaghan J, Streete P, Jones AL, Dargan PI (2006) Crit Care 10:R44
6. Zambakjian C, Sakur AA (2020) Future J Pharm Sci 6:110
7. Waraksa E, Wójtowicz-Zawadka M, Kwiatkowska D, Jarek A, Małkowska A, Wrzesień R, Namieśnik J (2018) J Pharm Biomed Anal 152:279
8. Yuvali D, Narin I, Soylak M, Yilmaz E (2020) J Pharm Biomed Anal 179:113001
9. Alsaad AAA, Alassadi EAS, Al-Salman HNK, Hussein HH (2019) Asian J Pharm 13:141
10. Ragab MAA, Abdel-Hay MH, Ahmed HM, Mohyeldin SM (2019) J Chromatogr Sci 57:592
11. Borahan T, Unutkan T, Şahin A, Bakırdere S (2019) J Sep Sci 42:678
12. Han Z, Lu L, Wang L, Yan Z, Wang X (2017) Chromatographia 80:1353
13. Naghdi E, Fakhari AR, Ghasemi JB (2020) J Iran Chem Soc 17:1467
14. Salem YA, Hammouda MEA, Abu El-Enin MA, El-Ashry SM (2019) Spectrochim Acta A Mol Biomol Spectrosc 210:387
15. Aydoğmuş Z, Asfoor A (2022) Chin J Anal Chem 50:100063
16. Kalambate PK, Noiphung J, Rodthongkum N, Larpant N, Thirabowonkitphithan P, Rojanarata T, Hasan M, Huang Y, Laiwattanapaisal W (2021) TrAC Trends Anal Chem 143:116403
17. Safaei M, Shishehbore MR (2021) Talanta 329:122247
18. Stojanović ZS, Đurović AD, Ashrafi AM, Koudelková Z, Zítka O, Richtera L (2020) Sens Actuators B Chem 318:128141
19. Stojanović Z, Đurović A, Kravić S, Grahovac N, Suturović Z, Bursić V, Vuković G, Brezo T (2016) Anal Methods 8:2698
20. Anzar N, Hasan R, Tyagi M, Yadav N, Narang J (2020) Sens Int 1:100003
21. Wang J (2006) Analytical electrochemistry. Wiley, Hoboken, NJ
22. Bard Allen J, Faulkner Larry R (2000) Electrochemical methods: fundamentals and applications, 2nd edn. Wiley, New York, NY
23. Stoytcheva M, Zlatev R, Velkova Z, Gochev V, Valdez B, Kirova G, Hristova Y (2022) Int J Electrochem Sci 17:220668
24. Mutharani B, Rajakumaran R, Chen SM, Ranganathan P, Chen TW, Farraj DAA, Ali MA, Al-Hemaid FMA (2020) Microchem J 159:105378
25. Apetrei IM, Bejinaru AA, Boev M, Apetrei C, Buzia OD (2017) Farmacia 5:790
26. Đurović A, Stojanović Z, Bytešníková Z, Kravić S, Švec P, Přibyl J, Richtera L (2022) J Mater Sci 57:5533
27. Svancara I, Kalcher K, Walcarius A, Vytras K (2012) Electroanalysis with carbon paste electrodes. CRC Press
28. Gosser KD (1993) Cyclic voltammetry simulation and analysis of reaction mechanisms. VCH, Weinheim
29. Laviron E (1974) J Electroanal Chem Interfacial Electrochem 52:355
30. Švorc Ľ, Strežová I, Kianičková K, Stanković D, Otřísal P, Samphao A (2018) J Electroanal Chem 822:144
31. (1995) ICH Topic Q 2 (R1) validation of analytical procedures: text and methodology. In: European Medicines Agency. https://www.ema.europa.eu/en/documents/scientific-guideline/ich-q-2-r1-validation-analytical-procedures-text-methodology-step-5_en.pdf. Accessed 6 June 2022

32. Đurović A, Stojanović Z, Kravić S, Kos J, Richtera L (2020) Electroanalysis 32:741
33. Hayat EO, Aamor M, Mustapha O, Mohamed M, Haimouti EL, Tarik EO (2022) Anal Bioanal Electrochem 14:18
34. Rivera-Hernández SI, Álvarez-Romero GA, Corona-Avendaño S, Páez-Hernández ME, Galán-Vidal CA, Romero-Romo M (2016) Instrum Sci Technol 44:483
35. Loudiki A, Boumya W, Hammani H, Nasrellah H, Bouabi YE, Zeroual M, Farahi A, Lahrich S, Hnini K, Achak M, Bakasse M, El Mhammedi MA (2016) Mater Sci Eng C 69:616
36. Loudiki A, Hammani H, Boumya W, Lahrich S, Farahi A, Achak M, Bakasse M, El Mhammedi MA (2016) Appl Clay Sci 123:99
37. Panić S, Rakić D, Guzsvány V, Kiss E, Boskovic G, Kónya Z, Kukovecz Á (2015) Chemosphere 141:87
38. Ratkovic S, Vujicic D, Kiss E, Boskovic G, Geszti O (2011) Mater Chem Phys 129:398
39. Azadi P, Farnood R, Meier E (2010) J Phys Chem A 114:3962
40. Liu S, Yan Z, Zhang Y, Wang R, Luo SZ, Jing F, Chu W (2018) ACS Sustain Chem Eng 6:14403